IOPscience iopscience.iop.org

Home Search Collections Journals About Contact us My IOPscience

Differential cross sections for vibrational excitation of CO_2 by 1.5-30 eV electrons

This article has been downloaded from IOPscience. Please scroll down to see the full text article.

2001 J. Phys. B: At. Mol. Opt. Phys. 34 1929

(http://iopscience.iop.org/0953-4075/34/10/308)

View the table of contents for this issue, or go to the journal homepage for more

Download details:
IP Address: 203.230.125.100
The article was downloaded on 01/06/2011 at 06:18

Please note that terms and conditions apply.

INSTITUTE OF PHYSICS PUBLISHING JOURNAL OF PHYSICS B: ATOMIC, MOLECULAR AND OPTICAL PHYSICS

J. Phys. B: At. Mol. Opt. Phys. **34** (2001) 1929–1940 www.iop.org/Journals/jb PII: S0953-4075(01)20802-5

Differential cross sections for vibrational excitation of CO_2 by 1.5–30 eV electrons

M Kitajima[1], S Watanabe[1], H Tanaka[1], M Takekawa[2], M Kimura[3] and Y Itikawa[4]

[1] Department of Physics, Sophia University, Tokyo 102-8554, Japan
[2] RIKEN, Saitama 351-0198, Japan
[3] Graduate School of Science and Engineering, Yamaguchi University, Yamaguchi 755-8611, Japan
[4] Institute of Space and Astronautical Science, Kanagawa 229-8510, Japan

Received 11 January 2001

Abstract

A crossed-beam experiment has been performed to measure differential vibrationally inelastic cross sections for electron scattering from CO_2 in the energy range from 1.5 to 30 eV over the scattering angles of 10–130°. Near the $^2\Pi_u$ resonance at 3.8 eV, the angular and energy dependences of the differential cross sections (DCS) have been determined in detail. Absolute values are obtained by normalizing the inelastic cross sections to the elastic ones. To determine the intensity of the individual vibrational modes from the energy-loss spectra, a deconvolution procedure was employed. The DCS for the pure fundamental modes (010), (100), (001) and the overtone of (020) are reported in detail for the first time over wide ranges of impact energy and scattering angle.

1. Introduction

As part of a planned programme, efforts have been underway to determine quantitatively the electron collision cross sections of carbon dioxide, such as the differential cross sections (DCSs) for elastic scattering (Tanaka *et al* 1998) and vibrational (this work) and electronic excitations (Kitajima *et al* 2001). Nakamura (1995) has determined the integral cross section set for CO_2 by electron impact by using swarm analysis over the electron impact energies from 0.1 to 100 eV. The available data for that analysis, however, have been limited and fragmentary in the inelastic collision processes, hence his recommended data-set is still somewhat controversial. Moreover, there is a considerable amount of variation in the available absolute values even for both total and elastic scattering integral cross sections (Kimura *et al* 1997). The purpose of this paper is to investigate differential cross sections for CO_2 vibrational excitation by electrons with impact energies of 1.5, 2.0, 3.0, 3.5, 3.8, 4.0, 4.5, 5.0, 6.0, 15 and 30 eV in more detail. The present measurements overlap with the previous results (Register *et al* 1980, Kochem *et al* 1985, Antoni *et al* 1986, Johnstone *et al* 1995) at some impact energies, but were intended to be systematic and comprehensive in their own right. Moreover, whilst the integral cross

0953-4075/01/101929+12$30.00 © 2001 IOP Publishing Ltd Printed in the UK

sections for each vibrational mode around the shape resonance centred at 3.8 eV have been discussed elsewhere (Kitajima *et al* 2000), the DCSs have not yet been presented in detail. These quantitative DCS data are quite essential for the basic assessment of collision theory as well as for the modelling performed in other areas, for example, discharge phenomena, upper atmospheric processes and astrophysics.

Carbon dioxide is a linear tri-atomic molecule of $^1\Sigma_g^+$ symmetry in its ground state. It has three normal modes of vibration, i.e. a bending mode ($0n0$) with Π_u symmetry, a symmetric stretching ($n00$) with Σ_g symmetry, and an asymmetric stretching ($00n$) with Σ_u symmetry, respectively. Needless to say, no dipole moment appears in the ground state of CO_2, but one is induced when either the bending or asymmetric stretching modes are excited. Thus, both of these modes are characterized by time-dependent dipole moments and, in general, are referred to as being infrared-active. The symmetric stretching mode is referred to as being Raman-active.

The total cross section of CO_2 by electron impact shows a resonant enhancement in the energy region of 2–5 eV, a sharp increase as you go to lower impact energies, and a broad hump near the ionization threshold at 11.5 eV. The resonant peak, centred at 3.8 eV, consists of elastic and inelastic scattering processes, because the lowest electronic excitation threshold is around 7 eV ($^3\Sigma_u^+$ state). Note that the resolution of the present spectrometer cannot resolve the rotationally excited states.

This resonance feature has been studied extensively many times over the past few years, and both previous experimental and theoretical studies were summarized by Currell and Comer (1993) and Johnstone *et al* (1995). Briefly, detailed investigations of the vibrational excitation and angular dependence of electron scattering have been performed by Andrick *et al* (1969), Boness and Schulz (1974) and Cadez *et al* (1974). Theoretically, the energy location of the peaks in their excitation functions was interpreted by the boomerang model (Birtwistle and Herzenberg 1971, Dubé and Herzenberg 1979, Hazi *et al* 1981, McCurdy and Turner 1983). Moreover, the structure near the threshold of vibrational excitations in CO_2 has been investigated by Kochem *et al* (1985), the rotational excitation and de-excitation cross sections by Antoni *et al* (1986), and scattering from vibrationally excited CO_2 by Johnstone *et al* (1995, 1999), respectively. The role of the Fermi resonance, in which the proximity of the vibrational modes (100) and (020) generates strong mixing between them, has been discussed by Currell and Comer (1993) and Johnstone *et al* (1995). Moreover, Cartwright and Trajmar (1996) proposed a model in which vibrational excitation of odd numbers of bending vibrational quanta by electron impact in the 3.5–5 eV energy region contains contributions from one or more core-excited (Feshbach) resonances rather than being produced entirely by boomerang resonance mechanisms.

In contrast, however, experimental vibrationally inelastic DCS have been limited to two measurements for the impact energies above 4 eV. One was performed by Register *et al* (1980) for scattering angles from 10° to 140° and at impact energies of 4, 10, 20 and 50 eV, and the other by Johnstone *et al* (1995) for only one scattering angle (20°) in the energy region from 1 to 7.5 eV. Thus, the available data are still fragmentary and, from a practical point of view, more cross section measurements are needed for a database for CO_2. The integral cross section sets for the three fundamental modes of vibrational excitation, as determined by Nakamura (1995), have been characterized as follow. Above 10 eV, the cross section for both the symmetric stretching (100) and bending (010) modes decreased steeply in magnitude compared with the asymmetric stretching (001) mode. In the lower-energy region below 2 eV, the magnitudes for the three cross sections for those modes were comparable with each other. Between 2 and 5 eV, the cross section for the (001) mode did not show any resonant enhancement, but the other two modes were clearly enhanced.

From a theoretical perspective, within the confines of vibrational excitation, there have been calculations using the dipole approximation (Itikawa 1971), an adiabatic nuclear-vibration approximation (Morrison *et al* 1977, Morrison and Lane 1979, Morrison and Hay 1979, Whitten and Lane 1982, Morrison 1999), and more recently using a vibrational two-state close-coupling scheme (Takekawa and Itikawa 1998, 1999).

2. Experimental

The experimental arrangement and procedures used in the present DCS measurements have been described in detail previously (Tanaka *et al* 1998). Briefly, the spectrometer consists of an electron gun with a hemispherical monochromator, a molecular beam and a rotatable detector with a second hemispherical system. Thus, the crossed-beam electron method is employed with the electron beam crossing an effusive molecular beam at right angles. A number of tube lenses in the spectrometer have been used for imaging and energy control of the electron beam, whose characteristics were confirmed carefully by electron trajectory calculations. To keep the transmission constant in the electron lens system, programmable power supplies control the driving voltages of some of the lenses. Both the monochromator and the analyser are enclosed in differentially pumped boxes to reduce the effect of background gases and to minimize the stray electron background. The target molecular beam is produced by effusing CO_2 through a simple nozzle with an internal diameter of 0.3 mm and length 5 mm. The spectrometer and the nozzle are heated to a temperature of about 50 °C to reduce contamination during the measurements. The analyser can be rotated around the scattering centre covering the angular range from -10° to 130° with respect to the incident electron beam.

During the present measurements, the overall energy and angular resolutions are 30–35 meV (FWHM) and about $\pm 1.5^\circ$, respectively, with a primary electron beam current of 3–7 nA. Furthermore, the voltages for both input and output lenses of the hemispheres were adjusted carefully to ensure that the base shape of the energy-loss spectra were as symmetric as possible. The present energy resolution is not sufficient to resolve the rotational excitations and adjacent vibrational bands of (020), the overtone for the (010) bending mode at 0.0827 eV, and (100) as well as (030), (110), (001), (040) and (120). The spectral decomposition with a least-squares fitting procedure is similar to that described earlier (Dillon *et al* 1993) and is employed to unfold the intensity of the individual modes. Briefly, apparatus functions for the fitting are estimated from the elastic DCS spectra of He and are assumed to be Gaussian profiles, which was found to give nearly the best fit to each energy-loss feature. Therein, the energy of the fundamental modes was referred to Shimanouchi (1972).

The scattering spectrometer is operated in two ways. For the measurements of the angular dependence for the excitation processes, the intensity of the scattered electron signal is counted as a function of energy loss at a fixed impact energy and scattering angle. To study resonances in vibrational excitations, for instance, excitation functions were measured in which the analyser is set to transmit only signals corresponding to a specific energy-loss channel as a function of impact energy. Although the resonance features around 3.8 eV have been studied extensively with excitation functions from the late 1970s to today, note that almost all the data may contain certain contributions from other vibrational modes. Even with the latest high-resolution capability of 10–15 meV, it is impossible to resolve their individual modes.

The energy-loss spectra have been measured carefully in order to obtain sufficient intensity for each vibrational excitation peak. The incident electron energy is calibrated with respect to the 19.35 eV resonance of He and for vibrational excitations to the $^2\Pi_g$ resonances of N_2. Cross sections were normalized to the elastic cross section (Tanaka *et al* 1998) by using the measured inelastic-to-elastic intensity ratios. Experimental errors are estimated to be 15–20% for elastic

DCSs and 30% for vibrational excitation cross sections, inclusive of errors in deconvolving the intensity of the individual vibrational modes from the energy-loss spectra (5%).

3. Results and discussion

Typical energy-loss spectra that have been measured at scattering angles of 20°, 70° and 120°, for an impact energy of 4.0 eV, are presented in figure 1. Figure 2 shows energy-loss spectra obtained at impact energies of 2.0, 3.8 and 5.0 eV for a scattering angle of 110°. At the impact energies of 3.8 and 4.0 eV, around the $^2\Pi_u$ shape resonance where elastic scattering is also enhanced, many higher vibrational harmonics appear strongly. On the other hand, only the fundamental modes can be observed in the energy-loss spectra at 2.0 eV. At 5.0 eV, the spectra differ from those of 2.0 eV, especially for the bending mode. The energy-loss peak at 0.16 eV consists of two excitation processes, i.e. an overtone of the bending mode at 0.159 eV (020) and the fundamental of the symmetric stretching mode at 0.172 eV (100). In figure 3, the deconvolved fit of the vibrational excitation peaks is shown at the impact energy of 3.5 eV for the scattering angle of 80°. As mentioned above, the energy-loss spectra have been carefully fitted with a Gaussian lineshape which is nearly identical to that for the He elastic peak. In figures 1–3, the peak positions are indicated by the insets and considerable overlapping mode structure is recognized especially in the energy-loss regions from 0.2 to 0.4 eV.

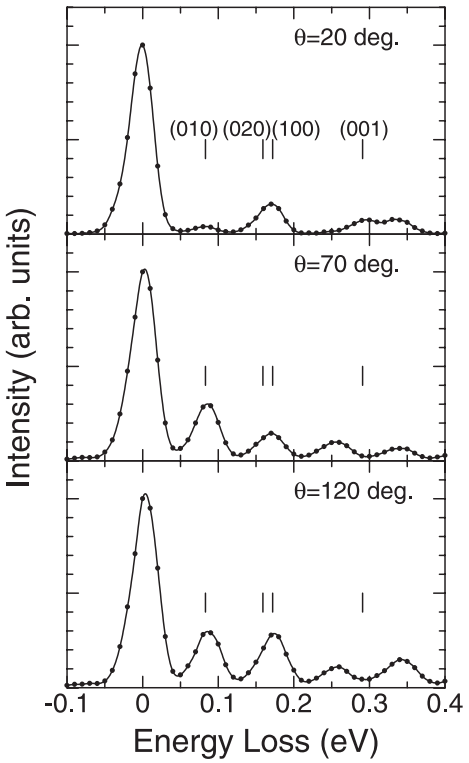

Figure 1. Electron energy-loss spectra in CO_2 at 4 eV incident electron energy for the scattering angles of 20, 70 and 120°.

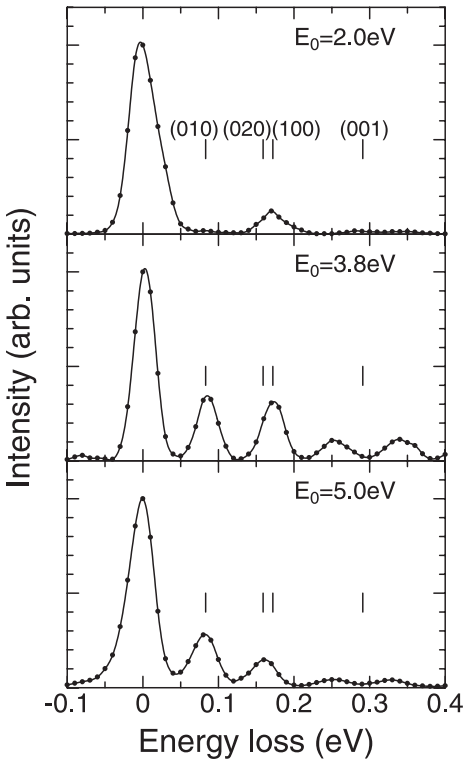

Figure 2. Electron energy-loss spectra in CO_2 at a scattering angle of 110° for the impact energies of 2, 3.8 and 5 eV.

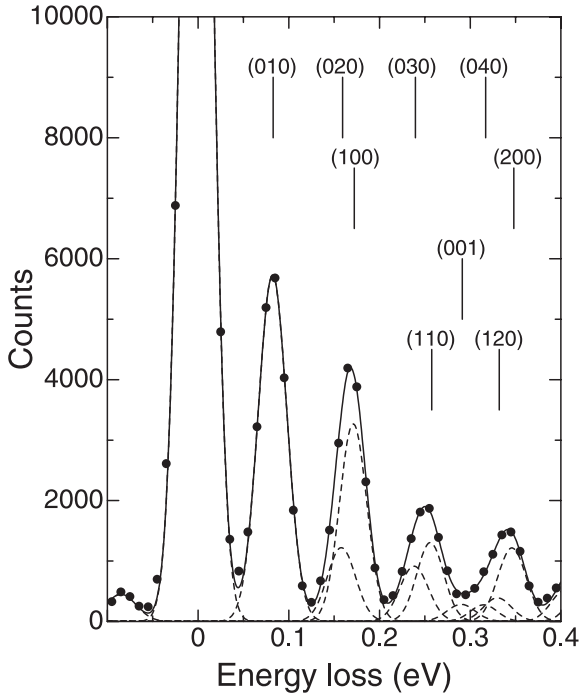

Figure 3. The deconvolved overlapping mode structure for the electron energy-loss spectrum in CO_2 at 3.5 eV incident electron energy and at a scattering angle of 80°.

To confirm the resonance positions, the excitation functions for the 0.083, 0.16 and 0.29 eV energy losses were also measured. A respective example of these measurements is shown in figure 4. These DCSs were normalized to those for He by means of the relative-flow method. Enhancements appear at 3.8, 10 and 30 eV, respectively, the first of which has been investigated extensively and ascribed undoubtedly to the resonance of symmetry $^2\Pi_u$. This resonance forms when the incident electron is trapped in the $2\pi_u$ molecular orbital, i.e. a temporary negative ion is formed. Due to the zero derivative around a bending angle of 180° in the potential energy curves of CO_2 and CO_2^-, the bending motion occurs much more slowly than the molecular stretches during the lifetime of the negative ion. This difference is reflected in the Franck–Condon overlapping between the negative ion and the neutral CO_2, and thus leads to enhancements of the symmetric stretching modes while only one or two bending modes are excited. Therefore, the bending motion can be ignored in the boomerang model. Johnstone *et al* (1995), however, claimed that this theory would not explain the abnormally large cross sections for the (020), (040) and (120) modes. A detailed discussion on the role of the Fermi resonances can be found later (see section 3.2).

The final two resonances have been observed by Tronc *et al* (1979) and theoretically verified by the continuum multiple-scattering (CMS) calculation of Lynch *et al* (1979) to be associated with the σ_u and σ_g shape resonances. More recently, Takekawa and Itikawa (1998, 1999) confirmed all of these resonances by a vibrational two-state close-coupling theory, although there are still disagreements in respect to the position of resonance energies.

The theoretical study is based on the vibrationally two-state (i.e. the ground and the first excited states for each vibrational mode) close-coupling method with the fixed-nuclear

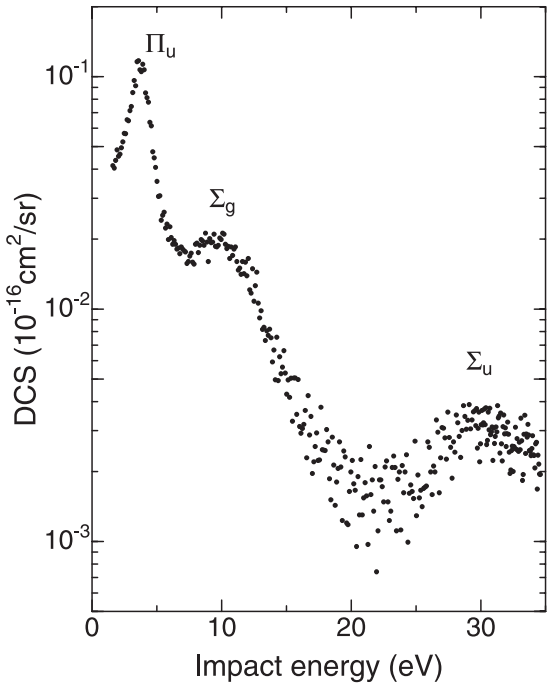

Figure 4. Absolute cross section for the excitation of the composed (020) and (100) vibrational modes of CO_2 by electron impact at 90°.

orientation (FNO) approximation. The interaction between the incident electron and the target molecule is composed of three terms, i.e. static, exchange and correlation–polarization potentials. The electrostatic potential is evaluated with a self-consistent field (SCF) target wavefunction. The exchange and the correlation–polarization interactions are approximately taken into account with a free electron gas model.

Figures 5(*a*)–(*d*) and tables 1–4 show the DCSs for vibrational excitations of (010), (020), (100) and (001) modes at several electron energies. Comparisons with the available experimental and theoretical data are also given in these figures. The experimental data of the present measurements are covered in the energy region 1.5–30 eV with scattering angles from 15° to 130°. Note that the unpublished data by Danner (1970) are excluded from the comparison. Note also that our corresponding integral and momentum transfer cross sections are excluded in this report around the resonance region of 3.8 eV. This is because that work was described in detail in our recent paper (Kitajima *et al* 2000). The primary objective of this report is to discuss the angular dependence in individual vibrational excitations by electron impact for the first time.

3.1. The bending mode, (010)

As shown in figures 1–3, the energy resolution for the present measurements was 30–35 meV, which provided good separation of the 0.083 eV energy-loss feature from the elastic peak. However, at the higher energies of 15 and 30 eV, additional care was also taken in adjusting the voltages of the lenses near the hemispheres to ensure that a long tail on the high-energy side of the elastic peak was minimized.

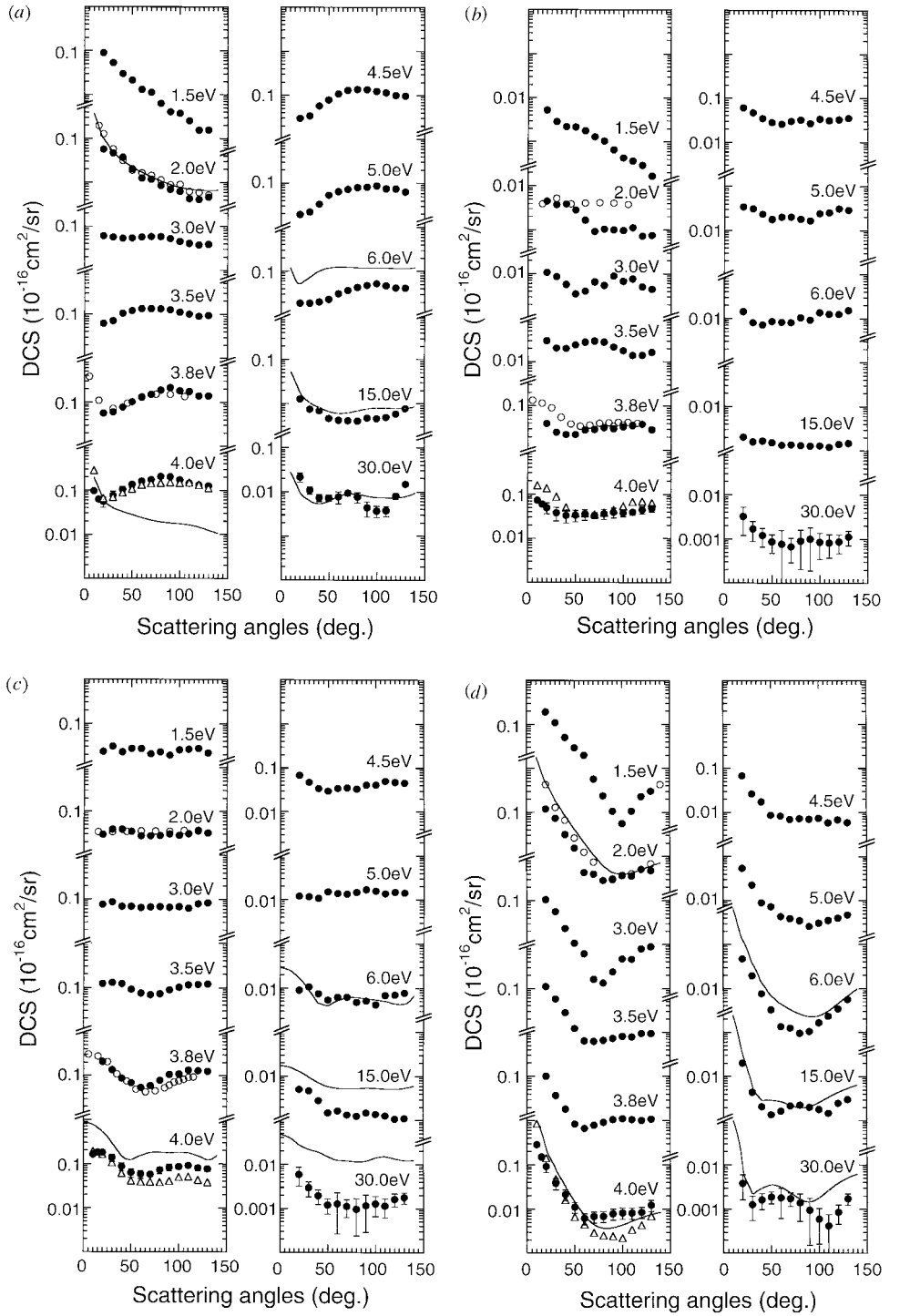

Figure 5. Absolute differential cross sections of: (*a*) (010), (*b*) (020), (*c*) (100) and (*d*) (001) vibrational excitation of CO_2 at electron impact energies from 1.5 to 30 eV; ●, present data; ○, Antoni *et al* (1986); △, Register *et al* (1980); ——, theoretical study of Takekawa and Itikawa (1998, 1999).

Table 1. Observed differential cross sections (10^{-16} cm^2 sr^{-1}) for vibrational excitation of the (010) mode of CO_2.

	Impact energy (eV)										
θ (deg)	1.5	2.0	3.0	3.5	3.8	4.0	4.5	5.0	6.0	15	30
10						0.0960					
15						0.0620					
20	0.0895	0.0565	0.0601	0.0621	0.0562	0.0547	0.0298	0.0194	0.0189	0.0126	0.0212
30	0.0531	0.0465	0.0568	0.0714	0.0599	0.0762	0.0338	0.0222	0.0189	0.0074	0.0108
40	0.0304	0.0371	0.0532	0.1049	0.0767	0.1039	0.0571	0.0336	0.0202	0.0069	0.0073
50	0.0214	0.0203	0.0537	0.1211	0.1022	0.1336	0.0783	0.0533	0.0230	0.0046	0.0072
60	0.0132	0.0125	0.0567	0.1339	0.1289	0.1596	0.1083	0.0646	0.0309	0.0042	0.0076
70	0.0113	0.0117	0.0579	0.1340	0.1516	0.1719	0.1305	0.0730	0.0368	0.0041	0.0093
80	0.0063	0.0085	0.0582	0.1330	0.1872	0.2048	0.1355	0.0796	0.0431	0.0040	0.0075
90	0.0041	0.0070	0.0523	0.1265	0.2144	0.2011	0.1348	0.0816	0.0479	0.0047	0.0043
100	0.0037	0.0063	0.0450	0.1121	0.1822	0.1705	0.1225	0.0869	0.0527	0.0045	0.0036
110	0.0025	0.0043	0.0406	0.1012	0.1754	0.1446	0.1149	0.0749	0.0474	0.0049	0.0037
120	0.0016	0.0041	0.0374	0.0905	0.1395	0.1295	0.0995	0.0745	0.0422	0.0058	0.0080
130	0.0016	0.0047	0.0391	0.0945	0.1391	0.1243	0.0969	0.0634	0.0414	0.0077	0.0148

Table 2. Observed differential cross sections (10^{-16} cm^2 sr^{-1}) for vibrational excitation of the (020) mode of CO_2.

	Impact energy (eV)										
θ (deg)	1.5	2.0	3.0	3.5	3.8	4.0	4.5	5.0	6.0	15	30
10						0.0728					
15						0.0594					
20	0.0053	0.0045	0.0106	0.0301	0.0399	0.0489	0.0603	0.0346	0.0144	0.0020	0.0032
30	0.0029	0.0038	0.0086	0.0206	0.0252	0.0375	0.0467	0.0311	0.0080	0.0016	0.0017
40	0.0022	0.0039	0.0057	0.0200	0.0226	0.0329	0.0347	0.0233	0.0071	0.0017	0.0012
50	0.0021	0.0029	0.0035	0.0244	0.0225	0.0334	0.0281	0.0178	0.0085	0.0015	0.0009
60	0.0018	0.0016	0.0040	0.0280	0.0284	0.0351	0.0256	0.0200	0.0082	0.0013	0.0008
70	0.0013	0.0009	0.0065	0.0298	0.0296	0.0330	0.0301	0.0201	0.0081	0.0014	0.0007
80	0.0010	0.0010	0.0055	0.0281	0.0323	0.0361	0.0323	0.0181	0.0105	0.0013	0.0009
90	0.0007	0.0010	0.0088	0.0218	0.0304	0.0388	0.0267	0.0165	0.0093	0.0013	0.0010
100	0.0004	0.0010	0.0068	0.0179	0.0336	0.0376	0.0338	0.0242	0.0137	0.0013	0.0009
110	0.0004	0.0011	0.0076	0.0140	0.0366	0.0390	0.0312	0.0253	0.0126	0.0012	0.0008
120	0.0003	0.0007	0.0051	0.0141	0.0384	0.0442	0.0326	0.0315	0.0125	0.0014	0.0009
130	0.0002	0.0007	0.0045	0.0165	0.0290	0.0480	0.0356	0.0289	0.0154	0.0015	0.0011

At impact energies of 1.5 and 2.0 eV, just below the resonance, i.e. off-resonance, figure 5(*a*) shows that the DCSs of the bending mode have strong forward peaks. For the bending mode, previous measurements of the DCSs (Kochem *et al* 1985, Antoni *et al* 1986) showed that the dipole interaction is responsible for the steep forward increase in the cross section in the low-energy region. All of these measurements provided evidence that the first-order Born approximation for the scattering of an electron at a point dipole potential (Itikawa 1971) gave accurate values for small scattering angles, even in the resonance region. As a result this theory has previously been used as follows: to extrapolate the inaccessible DCS between 0° and 20°, or 130° and 180° in order to obtain the integral and momentum transfer cross sections; and to place an absolute scale on the DCS with the transition dipole moment of the infrared-active modes (010) and (001) deduced from optical measurements (Bishop and

Table 3. Observed differential cross sections (10^{-16} cm^2 sr^{-1}) for vibrational excitation of the (100) mode of CO_2.

	Impact energy (eV)										
θ (deg)	1.5	2.0	3.0	3.5	3.8	4.0	4.5	5.0	6.0	15	30
10						0.1622					
15						0.1813					
20	0.0232	0.0295	0.0755	0.1232	0.2073	0.1783	0.0678	0.0120	0.0090	0.0050	0.0059
30	0.0307	0.0387	0.0868	0.1294	0.1357	0.1360	0.0472	0.0117	0.0106	0.0046	0.0029
40	0.0227	0.0387	0.0684	0.1221	0.0863	0.0872	0.0342	0.0108	0.0074	0.0028	0.0019
50	0.0271	0.0346	0.0683	0.0913	0.0682	0.0623	0.0297	0.0151	0.0054	0.0015	0.0012
60	0.0268	0.0274	0.0638	0.0746	0.0538	0.0582	0.0345	0.0138	0.0062	0.0016	0.0013
70	0.0205	0.0274	0.0662	0.0687	0.0591	0.0574	0.0352	0.0133	0.0062	0.0013	0.0011
80	0.0227	0.0280	0.0674	0.0719	0.0784	0.0721	0.0334	0.0147	0.0047	0.0012	0.0010
90	0.0192	0.0302	0.0653	0.0880	0.1069	0.0822	0.0411	0.0169	0.0051	0.0015	0.0012
100	0.0255	0.0284	0.0670	0.1020	0.1096	0.0863	0.0411	0.0159	0.0042	0.0014	0.0013
110	0.0260	0.0306	0.0620	0.1154	0.1330	0.0915	0.0502	0.0137	0.0069	0.0013	0.0011
120	0.0272	0.0359	0.0784	0.1179	0.1296	0.0806	0.0475	0.0148	0.0070	0.0011	0.0016
130	0.0215	0.0320	0.0825	0.1208	0.1260	0.0770	0.0457	0.0143	0.0078	0.0011	0.0018

Table 4. Observed differential cross sections (10^{-16} cm^2 sr^{-1}) for vibrational excitation of the (001) mode of CO_2.

	Impact energy (eV)										
θ (deg)	1.5	2.0	3.0	3.5	3.8	4.0	4.5	5.0	6.0	15	30
10						0.2859					
15						0.1501					
20	0.1914	0.1186	0.1047	0.1107	0.1008	0.0916	0.0671	0.0544	0.0471	0.0199	0.0038
30	0.1082	0.0733	0.0558	0.0576	0.0370	0.0379	0.0261	0.0225	0.0194	0.0044	0.0013
40	0.0503	0.0313	0.0231	0.0281	0.0182	0.0214	0.0172	0.0089	0.0076	0.0021	0.0016
50	0.0294	0.0154	0.0107	0.0122	0.0082	0.0111	0.0086	0.0072	0.0032	0.0014	0.0019
60	0.0197	0.0043	0.0061	0.0064	0.0067	0.0061	0.0082	0.0043	0.0013	0.0017	0.0018
70	0.0057	0.0040	0.0016	0.0062	0.0078	0.0068	0.0068	0.0039	0.0012	0.0022	0.0017
80	0.0024	0.0029	0.0013	0.0066	0.0091	0.0069	0.0072	0.0035	0.0010	0.0023	0.0014
90	0.0011	0.0031	0.0024	0.0072	0.0106	0.0078	0.0070	0.0026	0.0010	0.0020	0.0009
100	0.0006	0.0037	0.0047	0.0081	0.0110	0.0082	0.0073	0.0031	0.0016	0.0018	0.0006
110	0.0011	0.0036	0.0046	0.0079	0.0105	0.0081	0.0058	0.0035	0.0023	0.0015	0.0004
120	0.0023	0.0052	0.0079	0.0094	0.0100	0.0085	0.0067	0.0040	0.0034	0.0025	0.0009
130	0.0030	0.0048	0.0088	0.0094	0.0108	0.0123	0.0058	0.0047	0.0056	0.0030	0.0017

Cheung 1982). The present data accord substantially with the results from Antoni *et al* (1986) as well as with the Born theory at 2 eV.

Around the resonance region from 3 to 6 eV, the DCS behaviour shows more moderate (gentle) angular features with a broad maximum around 90° for angles above 30°. Note that such DCS features could be emphasized more clearly using a linear ordinate scale. At 3.8 and 4.0 eV, like the earlier measurements by Register *et al* (1980) and Antoni *et al* (1986), the present DCS indicate that the dipole interaction still dominates at low angles.

In general, a scattering process may be classified into direct (or non-resonant) and resonant terms, hence this dipole interaction corresponds to the former case. In the region of the $^2\Pi_u$ resonance, however, the scattering is described by both direct dipole interaction (dominant for $\theta \leqslant 20°$) and its interference with the resonance (dominant for $\theta \geqslant 30°$). Cartwright

and Trajmar (1996) suggested a possible contribution of a core-excited Feshbach resonance at 4–5 eV to the bending mode. By dividing the measured DCS at 4 eV into these two scattering processes and analysing them, they have derived the symmetry-forbidden argument for an odd number of vibrational quanta for the bending excitation. Therefore, DCSs for excitation into higher vibrational states have also been observed in this paper. However, the present findings show that there is no significant difference in bending-mode excitation for both the DCS and the partially integrated (20–130°) cross sections (Kitajima *et al* 2000).

Let us now consider figure 5(*a*) in more detail. Again all three data sets, although taken with different spectrometers (Register *et al* 1980, Antoni *et al* 1986), are in good agreement with each other. However, the recent calculation is unsatisfactory at 4 and 6 eV because of the resonant energy position being shifted to around 5 eV. Note here that the DCS calculated at 6 eV (Takekawa and Itikawa 1999) is similar in angular dependence but larger in magnitude when compared with the present data. The DCS becomes almost isotropic at 15 eV, with some growth towards 0°, and shows some undulation at 30 eV. The findings, however, accord reasonably with the theory at those energies. Further note, as mentioned above, although the resonance at 30 eV has been observed by Tronc *et al* (1979), its relative intensity was only determined in the DCS.

With the previous measurements at 10, 20 and 50 eV (Register *et al* 1980), the present results at 15 and 30 eV also contributed to providing a comprehensive database for CO_2 (010) vibrational excitation in higher-energy regions.

3.2. The symmetric stretching mode and the overtone of the bending mode, (100) and (020)

As discussed previously, even with the excellent resolution of 10–15 meV, the close spacing in energy of the overtone of the bending (020) (0.159 eV) and the stretching (100) (0.172 eV) modes means that they are not resolvable. Following our deconvolution procedure, figures 5(*b*) and 5(*c*) show the DCSs for the individual vibrational modes of (020) and (100).

For the (020) mode at 1.5 and 2 eV, the angular distributions are strongly forward peaked reflecting to the dipole interaction. This behaviour is similar to that seen in figure 5(*a*) for the fundamental bending mode at those energies. However, a tendency to undulation in the DCS is clearly visible within the experimental errors from 2 to 3.8 eV, inclusive of a small increase in the DCSs at lower angles. At higher energies from 4 to 15 eV, the DCSs become more isotropic and display the resonant characteristics of a weak d-wave, similar to the fundamental bending mode. Compared with the (010) DCSs, the (020) DCSs are less than 20% in overall magnitude except at 20°. At 2 eV, the present findings disagree with the DCS of Antoni *et al* (1986), but are in fair agreement with the previous results (Register *et al* 1980, Antoni *et al* 1986) at 3.8 and 4 eV, except for the forward scattering.

In the (100) mode, in contrast to the above two modes, (010) and (020), the DCSs are characterized notably by isotropic angular dependences. This is because of the non-dipole geometry in the symmetric stretching mode from 1.5 to 3 eV. Even with considerations for the direct processes via the interaction of the quadrupole potential (Breig and Lin 1965), including the polarization potential (Itikawa 1971), the experimental results (Kochem *et al* 1985) could not be explained within the first Born approximation below 2 eV. Thus the non-direct interaction mechanisms, based on the virtual state, have been expected to describe the excitation of the symmetric stretching mode, as investigated theoretically by Morrison and Lane (1979) and Whitten and Lane (1982). Around the resonance from 3.5 to 4.5 eV, the DCS shows certain features that were also found in the bending mode. In addition the DCSs show a decreasing trend in magnitude toward smaller angles around the 10–20° region, due to polarization effects and a shallow minimum around 60°. They also have a comparable magnitude with the (010)

mode. As shown in figure 5(*c*), the DCSs are again flattening out from 5 to 6 eV, and they exhibit some typical features, i.e. an increase in magnitude at small angles but the isotropic angular characteristics still dominate at larger angles as the impact energy increases. The present (100) DCSs agree with the previous results of Antoni *et al* (1986) at 2.0 and 3.8 eV, as well as with that of Register *et al* (1980) at 4.0 eV, excluding some minor discrepancies above 40°. Recent calculations from Takekawa and Itikawa (1998, 1999) are expected to be different in magnitude, but agree quite reasonably with the shape of the angular distributions except for an unusual case at 6.0 eV.

As mentioned above, the role of the Fermi resonance in which the vibrational modes (100) and (020) being very close in energy experience strong mixing has been discussed by both Currell and Comer (1993) and Johnstone *et al* (1995). These two states are termed a diad. They have noted that due to the strong mixing in the diad, an individual mode cannot be considered as being pure symmetric stretch or pure bend. For a particular polyad of higher values of $n = 6$, the shifting in the energy-loss peak positions was found to be as much as 25 meV, especially at higher angles (65°), as the resonance region was traversed (Currell and Comer 1993). Furthermore, abnormally large cross sections for the (020), (040) and (120) modes were observed at 20°, which were not explained by the boomerang model (Johnstone *et al* 1995). In the present measurements, the diad state was the lowest of the vibrational modes (100) and (020) and unlike the findings of Johnstone *et al*, no such anomaly was observed within the (020) mode only, except for an extreme case at 20°. Therefore, the role of the Fermi resonance, which causes further complications in situations where it is not being studied explicitly, has been avoided in the present analysis of the diad.

3.3. The asymmetric stretching mode, (001)

Figure 5(*d*) shows that the structures and undulations in the DCS for the (001) mode vary continuously and systematically as a function of the impact energy and scattering angle. There is no significant feature due to the resonance around 3.8 eV, unlike the other modes.

At 1.5 eV, the DCS also shows a steep increasing trend in magnitude as the scattering angle decreases. A local minimum appears at 100° followed again by an increase, although with a very small DCS magnitude. The sharp increases in the DCS toward smaller angles for the (001) mode are due to the dipole moment as already mentioned above for the (010) mode. As the energy slightly increases to 3.8 eV, the cross section minimum shifts toward lower angles, and a plateau region emerges with a small local maximum at around 100°. This small maximum may be attributed to the resonance, but only very weakly. From 4 to 6 eV, the shape of the DCSs shows a steep increase at small angles and a sharp drop as the impact energy increases. As the impact energy reaches 15 and 30 eV, the DCS has two shallow dips at 30° and 110°. The present DCSs are in good agreement with the previous data except for larger angles at 4 eV. Furthermore, a vibrational two-state close-coupling theory reproduces the shape of the DCS very well.

Similar to the conclusions provided in the previous measurements (Register *et al* 1980, Kochem *et al* 1985, Antoni *et al* 1986), the present results verify that the bending and stretching modes resonance ($^2\Pi_u$) plays no significant role in exciting the Σ_u asymmetric stretching mode. Note here that the DCSs are very small in magnitude over all energy regions and scattering angles excluding the dipole forward peaks. However, further note that because many other modes are involved around the energy-loss peak of (001), as shown in figure 3, errors in deconvolving the intensity of the individual modes from the measured energy-loss spectra cannot be avoided in that case.

4. Conclusions

Inclusive of the previous measurements, the present results have provided a comprehensive and quantitative data set for the individual fundamental vibrational excitation modes of CO_2 over a wide range of impact energies and scattering angles. While many papers have been presented recently on electron collisions with CO_2, especially theoretical ones, these quantitative data also serve as a stringent test of the approximations used in the collision theories.

Acknowledgments

We are indebted to Professor S J Buckman and Dr R J Gulley for reading the manuscript and giving helpful suggestions. We also wish to thank Dr M J Brunger of Flinders University of South Australia for helpful comments on our manuscript. HT also gratefully acknowledges the warm hospitality extended to him by Professor S J Buckman during a sabbatical at the Australian National University, Canberra, where this paper was written.

References

Andrick A, Danner D and Ehrhardt H 1969 *Phys. Lett.* A **29** 326
Antoni Th, Jung K, Ehrhardt H and Chang E S 1986 *J. Phys. B: At. Mol. Phys.* **19** 1377
Birtwistle D T and Herzenberg A 1971 *J. Phys. B: At. Mol. Phys.* **4** 53
Bishop D M and Cheung L M 1982 *J. Phys. Chem. Ref. Data* **11** 119
Boness M J W and Schulz G J 1974 *Phys. Rev.* A **9** 1969
Breig L B and Lin C C 1965 *J. Chem. Phys.* **43** 3839
Cadez I, Tronc M and Hall R I 1974 *J. Phys. B: At. Mol. Phys.* **7** L132
Cartwright D C and Trajmar S 1996 *J. Phys. B: At. Mol. Opt. Phys.* **29** 1549
Currell F and Comer J 1993 *J. Phys. B: At. Mol. Opt. Phys.* **26** 2463
Danner D 1970 *PhD Thesis* Physikalisches Institute der Universitat Freiburg
Dillon M A, Boesten L, Tanaka H, Kimura M and Sato H 1993 *J. Phys. B: At. Mol. Opt. Phys.* **26** 3147
Dubé L and Herzenberg A 1979 *Phys. Rev.* A **20** 194
Hazi A U, Resigno T N and Kurilla M 1981 *Phys. Rev.* A **23** 1089
Itikawa Y 1971 *Phys. Rev.* A **3** 831
Johnstone W M, Akther P and Newell W R 1995 *J. Phys. B: At. Mol. Opt. Phys.* **28** 743
Johnstone W M, Brunger M J and Newell W R 1999 *J. Phys. B: At. Mol. Opt. Phys.* **32** 5779
Kimura M, Sueok O, Hamada A, Takekawa M, Itikawa Y, Tanaka H and Boesten L 1997 *J. Chem. Phys.* **107** 6616
Kitajima M, Ishikawa T, Tanaka H, Kimura M and Itikawa Y 2001 to be published
Kitajima M, Watanabe S, Tanaka H, Takekawa M, Kimura M and Itikawa Y 2000 *Phys. Rev.* A **61** 060701(R)
Kochem K-H, Sohn W, Hebel N, Jung K and Ehrhardt H 1985 *J. Phys. B: At. Mol. Phys.* **18** 4455
Lynch M G, Dill D, Siegel J and Dehmer J L 1979 *J. Chem. Phys.* **71** 4249
McCurdy C W and Turner J L 1983 *J. Chem. Phys.* **78** 6773
Morrison M A 1999 Private communication
Morrison M A and Hay P J 1979 *J. Chem. Phys.* **70** 4034
Morrison M A and Lane N F 1979 *Chem. Phys. Lett.* **66** 523
Morrison M A, Lane N F and Collins L A 1977 *Phys. Rev.* A **15** 2186
Nakamura Y 1995 *Aust. J. Phys.* **48** 357
Register D F, Nishinura H and Trajmar S 1980 *J. Phys. B: At. Mol. Phys.* **13** 1651
Shimanouchi T 1972 *Tables of Molecular Vibrational Frequencies (NBS Circular no 39)* (Washington, DC: US Govt Printing Office)
Takekawa M and Itikawa Y 1998 *J. Phys. B: At. Mol. Opt. Phys.* **31** 3245
——1999 *J. Phys. B: At. Mol. Opt. Phys.* **32** 4209
Tanaka H, Ishikawa T, Masai T, Sagara T, Boesten L, Takekawa M, Itikawa Y and Kimura M 1998 *Phys. Rev.* A **57** 1798
Tronc M, Azria R and Pauneau R 1979 *J. Physique* **40** L323
Whitten B L and Lane N F 1982 *Phys. Rev.* A **26** 3170